ECE 1511 Project Report

Heartbeat Filtering and Respiration Extraction using EMD

Yujing Duan	Siyu Zhang	Tianrun Lu
1010073938	1010403653	1005069701

Abstract

The electrocardiogram (ECG) signal is a biomedical signal used for the purpose of diagnosis of cardiovascular diseases. In the process of capturing ECG signal, a lot of distortions such as muscular contractions caused by breathing and other electronic interference would be appeared in the measurement. Therefore, denoising of ECG signal is a key to enhance the clinical evaluation. In this project, the empirical mode decomposition (EMD) method is going to be studied and investigated because of its ability to deal with turbulent signals such as ECG. Since breath signal is a major distortion in electrocardiographic signal and the breath signal itself has medical value, further investigation and exploration on extracting breath signal from ECG based on EMD algorithm have been carried out in this work.

Introduction

In today's data-driven world, there is a growing trend to collect extensive data across various fields, employing diverse models and algorithms for analysis and future prediction. However, not all phenomena lend themselves to straightforward modeling, as many are non-stationary and non-linear in nature. This is particularly evident in specialized fields like wind data analysis in laboratory wind-wave tunnels, seismological studies, and medical diagnostics, especially in the context of Electrocardiogram (ECG) signals. Empirical mode decomposition (EMD) is a popular method to deal with such non-linear and non-stationary signals. With the ability of carrying out multi-scale analysis, EMD is widely used in de-noising of ECG. This paper is going to provide some background information of ECG. Then, the algorithm of EMD is going to be explained in detail. After that, reproductions of representative experiments from the literature will be presented in order to study the functionality of this type of decomposition. Our project aims at extracting the baseline offset from the ECG signal to obtain the breath and "cleansed" heartbeat from the patient by utilizing the EMD algorithm and conducting complete or partial extraction for IMFs. The datasets used for analyzing that are from PhysioNet. The first dataset is abdominal and direct fetal ECG database, denoted as R dataset and the B dataset refers to the dataset called combined measurement of ECG, breathing and seismocardiograms.

Electrocardiogram (ECG)

ECG signals, which record the bioelectrical activity of the heart, are influenced by numerous physiological factors, and exhibit individual variability. These signals are inherently non-linear and non-stationary, making their analysis complex. A clear and accurate ECG recording is crucial for diagnosing various cardiac conditions, such as heart rhythm irregularities, myocardial infarction, and structural heart abnormalities. The foundation for modern ECG analysis was laid by Willem Einthoven (1860-1927), who used string galvanometers to record

the first precise and clinically useful ECG signals. He also established the standard ECG waveform nomenclature (P, Q, R, S, T waves), which reflects different electrical and mechanical events in the heart [2].

In modern biophysics, the heart's functionality is driven by electrical impulses from pacemaker cells, maintaining a regular heartbeat. These impulses sequentially stimulate cardiomyocytes, a process effectively captured by the standard 12-lead ECG. There are 10 electrodes placed on the limbs and chest to produce 12 distinct graphical views of the heart's electrical activity, the corresponding displayed ECG signals are in figure 1.1. Further to analysis of each part of the signals, used Lead II as an example. It connects an electrode on the right arm (negative) to one on the left leg (positive), measures the voltage difference between these points, providing insights into the heart's electrical behavior. The ECG trace comprises various phases of cardiac electrical activity. P waves, originating in the sinus node and moving towards the atrioventricular node, indicate atrial depolarization, resulting in a positive deflection in Lead II. Q waves, associated with the initial depolarization of the ventricular septum, typically produce a negative curve in Lead II. R waves, more pronounced during active left ventricular activity, create a significant positive curve. S waves, brief negative deflections, occur as bioelectricity travels counter to the lead's vector. T waves, representing ventricular repolarization, signal the heart muscle's return to its resting state. [4]

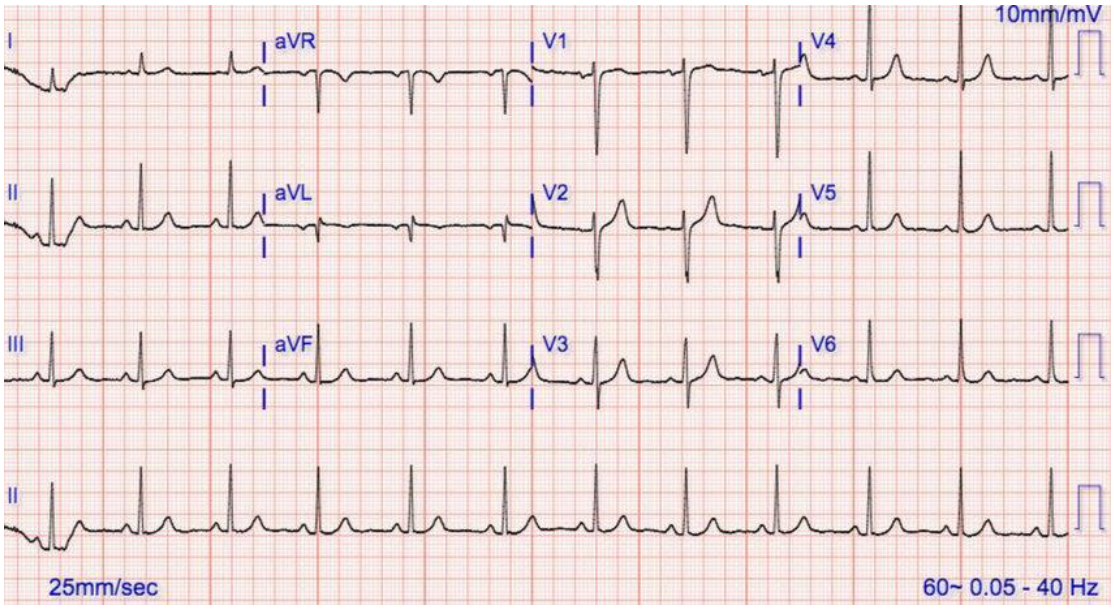

Figure 1.1. Repeat 12 lead Electrocardiogram (ECG or EKG), showing normal sinus rhythm. In the graph, the labels correspond to different electrode placements: the limb leads are divided into standard bipolar limb leads (I, II, and III) and augmented unipolar leads (aVL, aVF, and aVR), while the precordial leads are represented by V1 to V6. [3]

However, ECG recordings are often accompanied by several types of noise, such as baseline drift, powerline interference, electromyographic noise and other types of noise pollution. Here is a direct view of how the noise will interfere with the ECG signals in figure 1.2. Baseline drift, which is shown in figure 1.1, primarily caused by respiration and muscle movement, leads to a slow, gradual vertical shift in the ECG signal, known as baseline wander. In contrast, powerline

interference, typically at 50 Hz or 60 Hz (depending on the local power supply frequency), introduces high-frequency noise into the ECG trace. Electromyographic noise is typically characterized as high-frequency noise, usually above 100 Hz. It comes from the electrical activity of skeletal muscles. This interference becomes more pronounced when muscles near the ECG electrodes contract, as can happen during shivering, movement, or tension. Asking the patient to be quiet and relaxed during the ECG recordings can help physically reduce some of the noise. To mitigate these issues through the filter, ECG equipment often employs a combination of low-pass and band-stop filters before exporting the data. A low-pass filter, typically using a Butterworth or Chebyshev design with a 100 Hz cutoff frequency, is used to reduce high-frequency noise such as electromyographic noise. Then added a band-stop filter centered around 60 Hz to specifically target and eliminate power line interference, thereby enhancing the clarity of the crucial ECG components (P, Q, R, S, T waves). [5]

The power line interference and the electromyographic noise can be eliminated before exporting the data, but for the baseline wander needs further decomposition and analysis. There are many ways to solve the baseline wander, such as discrete wavelet transform, wavelet-based high-pass filtering, moving median and subtraction and empirical mode decomposition. For example, Discrete Wavelet Transform (DWT) uses Daubechies wavelet, it is effective, but it faces a significant drawback as it adheres to Nyquist's rule, leading to the loss of half the signal's frequency. This might cause the missing of partial sample data. [6] In the case of wavelet-based high-pass filtering, reconstructing the original signal might be a challenge, because the spectral content of the artifact overlaps with the dominant frequency of the heart rate under resting conditions. If only using moving median and subtraction this method, the ST phase will decrease, due to the strong ability of the high-pass filtering.[7] But if these methods are combined or used after others methods could provide a better result for reducing the baseline wander. Empirical mode decomposition (EMD) is a proficient algorithm for analyzing ECG signals. Besides EMD, there are many effective methods to solve this problem such as Ensemble Empirical Mode Decomposition (EEMD).

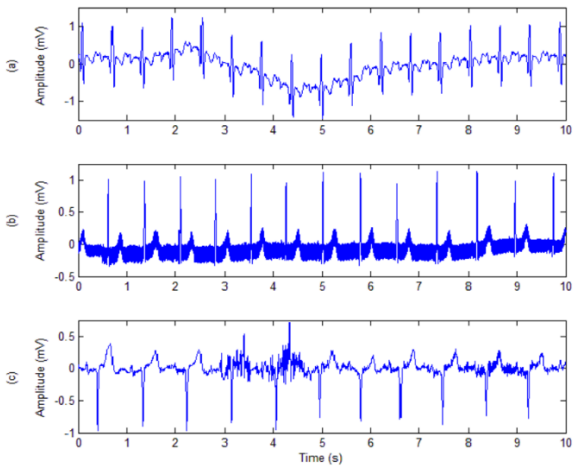

Figure 1.2. Common types of noise in ECG recordings. (a) Baseline wander. (b) 50 Hz power line interference, which presents as a regular and high-frequency disturbance and (c) Electromyographic noise, high-frequency spikes superimposed.

Empirical Mode Decomposition (EMD)

Empirical Mode Decomposition was proposed by Norden E. Huang and his coworkers in 1996. It is a powerful and versatile method for analyzing nonlinear and nonstationary data and does not use defined functions as a basis. Empirical Mode Decomposition has made substantial advancements in cardiac disease diagnosis, including the detection and forecasting of atrial fibrillation, characterized by irregular heart rhythms, and compromised blood flow. Additionally, it has proven effective in identifying and categorizing myocardial infarction, a critical heart condition that can result in tissue death and life-threatening consequences. Furthermore, it is instrumental in the prediction and prevention of sudden cardiac death.[8]
The fundamental concept of EMD involves breaking down the original signal into multiple Intrinsic Mode Functions (IMFs) and a residual, which represents the trend of the signal." Each IMF represents a simple oscillatory mode that is part of the data's decomposition with certain part of original frequency, and they are independent with each other. In other words, by combining all the IMFs across various time and frequency domains along with the residual component, the original signal can be accurately reconstructed. Every IMF is required to meet two conditions, firstly, the number of extrema (maxima and minima) and the number of the zero-crossings must either be equal or differ at most by one. The second is the mean value of the envelope defined by the local maxima and the envelope defined by the local minima is zero. Before extracting any IMFs, two assumptions must be met. The first assumption is that the signal possessing must have at least two extremal points: one maximum and one minimum. The second is that the characteristic timescale of the signal is determined by the interval between these two extreme points. To obtain IMFs, a process known as sifting is employed, which is iterative in nature. The initial step is to regard the starting signal as the first IMF, denoted by $X(t)$. The signal depicted in Figure 1.3 represents a combination of a tone and a chirp. A tone typically signifies a sound or signal with a constant frequency, while a chirp refers to a signal whose frequency either increases or decreases over time. The subsequent step involves identifying all local maxima and connecting them with a cubic spline to form the upper envelope, labeled as $X_{max}(t)$, represented by the blue line. Similarly, the lower envelope, $X_{min}(t)$, shown as the red line, is constructed by connecting all local minima using the same spline method. The mean of these two envelopes, depicted by the pink line in Figure 1.4, is calculated by the equation (1)

$$X_{mean1}(t) = \frac{X_{max}(t)+X_{min}(t)}{2} \quad (1)$$

The first residual signal, $d_1(t)$ is the result of original signal, $X(t)$ minus the mean value of current two envelopes, $X_{mean1}(t)$, the equation is

$$d_1(t) = X(t) - X_{mean1}(t) \quad (2)$$

At this stage, the signal must be tested to verify if it meets the two conditions necessary for an IMF. If the mean function $X_{mean1}(t)$ satisfies these conditions, then the signal $X(t)$ is designated as the first IMF resulting from the decomposition, which is called $c_1(t)$. The residual signal is $r_1(t)$. If $X_{mean1}(t)$ fails to meet the criteria, this indicates that the residual signal in figure 1.5, denoted as $d_1(t)$, requires further iteration. The process to determine the first IMF may involve several shifting. For this case, treating the residual signal, $d_1(t)$ as the

current signal $X(t)$. For this updated signal, the local maxima and minima are identified to construct the upper and lower envelopes, respectively. Subsequently, the mean envelope of the signal is calculated. Following this, the latest mean envelope is tested to determine whether it meets the predefined conditions for an IMF. Instead of using the two conditions to test whether it is IMF, the standard deviation (SD) would also be a method. It is calculated between the residue from the current iteration and the previous one, the two consecutive sifting. The standard deviation is shown in equation (3).

$$SD = \sum_{t=0}^{T} \frac{|d_{1(k-1)}(t) - d_{1k}(t)|^2}{d_{1(k-1)}^2(t)} \tag{3}$$

The termination of the shifting processing occurs when the standard deviation falls within a specific predefined range, usually set between 0.2 and 0.3. The small criterion helps the IMF to maintain the amplitude and frequency variation of the original signal. After n iteration, the residual signal is updated and gradually diminishes. The decomposition process concludes when the residual no longer exhibits significant oscillatory behavior or no more IMF can be extracted, which is the final residual, denoted as $r_n(t)$. The original signal can be reconstructed by summing all the IMFs obtained after n iterations along with the final residual and the equation is shown below.

$$X(t) = \sum_{i=1}^{n} c_i(t) + r_n(t) \tag{4}$$

Figure 1.6 illustrates the result of applying Empirical Mode Decomposition (EMD) to a signal, yielding six Intrinsic Mode Functions (IMFs) and one residual component. Generally, the initial IMFs represent the highest frequency oscillatory modes of the signal, while the succeeding IMFs capture progressively slower oscillations. This helps to analysis the signal in diverse frequency.

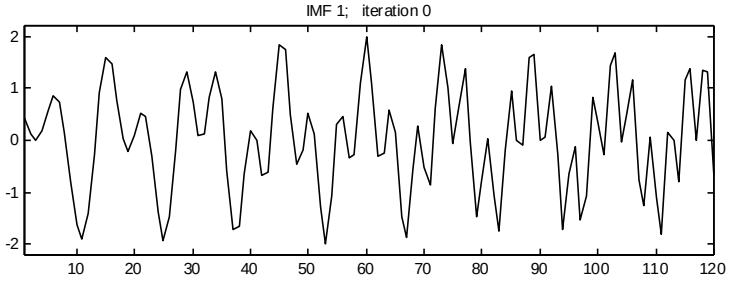

Figure 1.3. The original nonlinear and nonstationary signal, which is the combination of the tone and chirp. The original signal is regarded as the first IMF, $X(t)$.

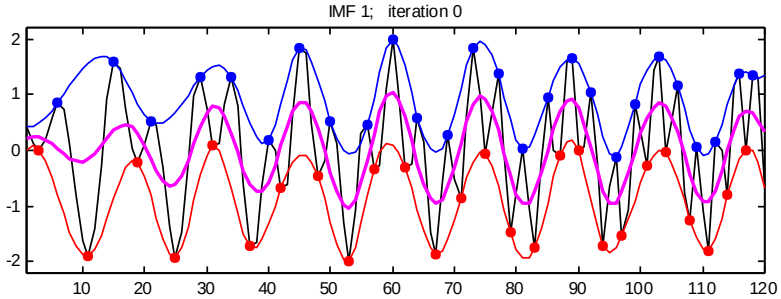

Figure 1.4. The blue points refer to the local maxima, and the red points refer to the local minima of the signal, $X(t)$. The blue line is the upper envelope, denoted as $X_{max}(t)$ and right line is the lower

envelope, denoted as $X_{min}(t)$. The pink line is the mean value of the two envelopes, $X_{mean}(t)$ by using the equation (1).

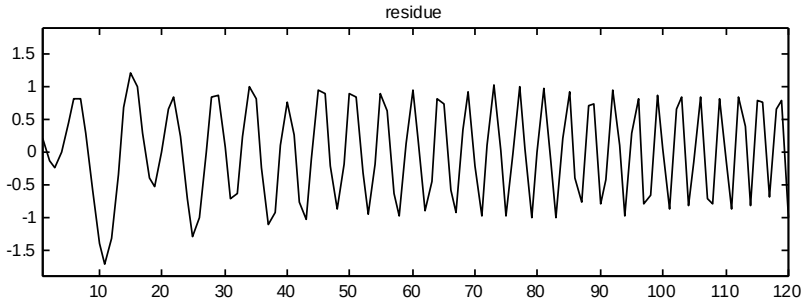

Figure 1.5. It shows the residue, $d_1(t)$ after the first iteration. Since the IMF does not meet the two conditions, the signal, $d_1(t)$ need the further analysis.

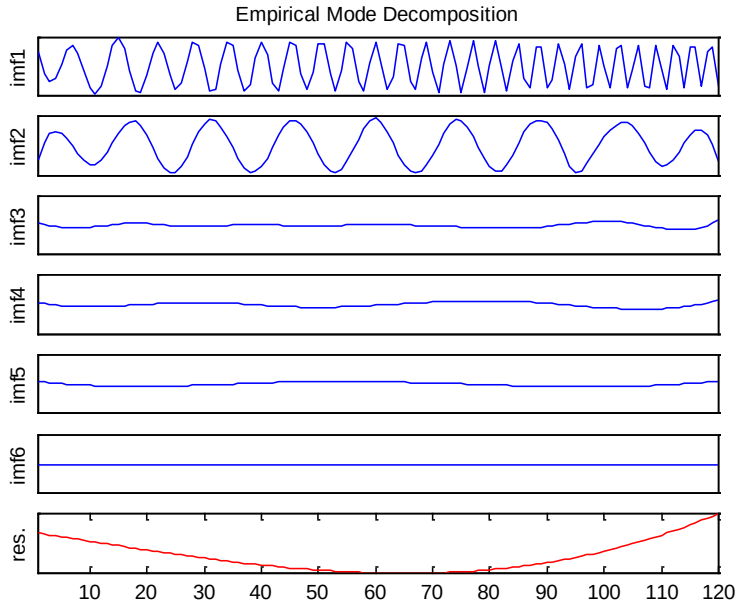

Figure 1.6. An example of the signal in figure 1.3 after empirical mode decomposition. It extracts 6 IMFs and a final residual.

Reproductions of experiments:

The EMD algorithm involves decomposing the signal into series of IMFs which are obtained from sifting process. During sifting, the local extrema is identified and then an envelope would be fitted to these extrema. The difference between the signal and its envelope is then computed and this process keeps repeating until a locally smooth IMF is found. The computed IMFs represent different oscillation or resolution scales in the input signal. The first IMF captures the highest frequency oscillations and the last IMF records the lowest frequency oscillation. The residual signal is the result of subtracting all IMFs from the input signal. And it represents the trend of the original signal.

A simple but effective example would be given first to demonstrate and visualize the functionality of empirical mode decomposition. The input signal x(t) involves a fast oscillation superimposed on a slower one.

$$x(t) = 5\,cos\left(\frac{2\pi}{10}t\right) + 10\,cos\left(\frac{2\pi}{200}t\right) \quad (5)$$

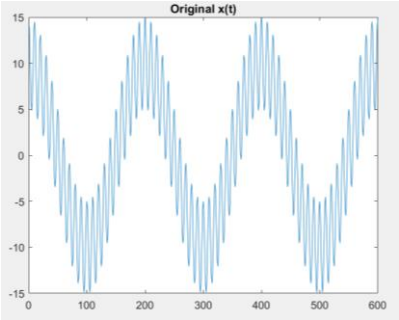

Figure 2.1. Input signal

Carrying out EMD on such input signal, the result is shown below.

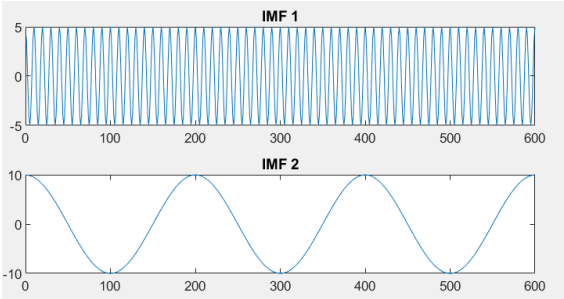

Figure 2.2. EMD results

The smallest time scales which mean the highest frequencies one can resolve are dictated by the time lap between successive extrema of the input data x(t). Since the first IMF is derived directly from the extrema of the original input signal, it contains the smallest timescales or the highest frequency. For finding IMF2, the same steps are repeated with the updated input signal which is the difference between original input x(t) and IMF1. Therefore, the second IMF must contain larger timescale comparing to the first IMF because the highest frequency component of original data is filtered out through updating the decomposition target. This is the reason that modes extracted by EMD are always ordered from high to low frequency content and why this iterated process is called sifting process. As shown in the results of EMD, IMF1 captures the first term in x(t) because it has higher frequency. The second term is being decomposed to the second mode. Therefore, IMF2 is equivalent to the second sinusoidal wave in the input signal. In this case, there are only different frequency components in the input signal. If there are more distinct frequency components, the process is going to be repeated until all IMFs are extracted according to the stop criterion and the residual is going to be almost a monotonic function in which no more meaningful extrema can be extracted.

In this case, there is no noise or interference attached to the original signal so the residual is very smooth and negligible small. If two components IMF1 and IMF2 are added together, the signal is successfully reconstructed.

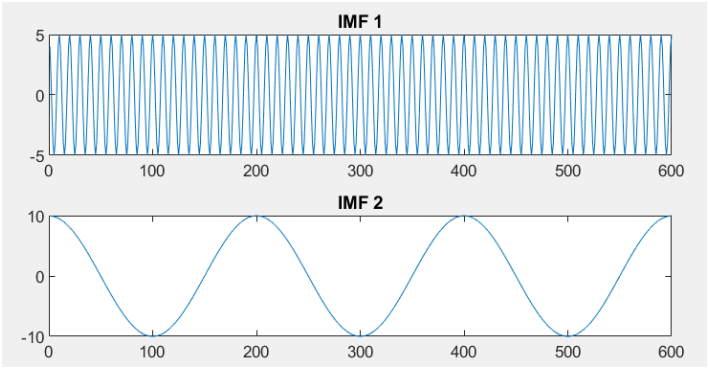

Figure 2.3. Reconstruction using IMFs

Hilbert transform, which is based on the fast Fourier transform, computes the minimum-phase response from the spectral perspective. It is capable of producing frequency response with linear-phase component being removed. There are several advantages of adapting Hilbert Transform in signal process. It involves the energy information of the input signal. It is consistent with the obtained frequency and time characteristics. Besides, it has high information content and ability to analyze the dynamics of changes in the characteristics of the input data. The captured characteristics can be used for assessing the power quality characteristics and monitoring the energy facilities [9]. Hilbert-Huang transform is a modified method decomposes input data into IMF, indicating the instantaneous frequency of the data. It is an efficient way to analyze nonstationary and nonlinear data. The following reproduction experiments results are going to be evaluated with the help of Hilbert-Huang transform for better spectral analysis on signals to identify localized features.

Firstly, the experiment of wind data from Huang's paper [10] is chosen to be reproduced as this is a good example to illustrate the sifting process.

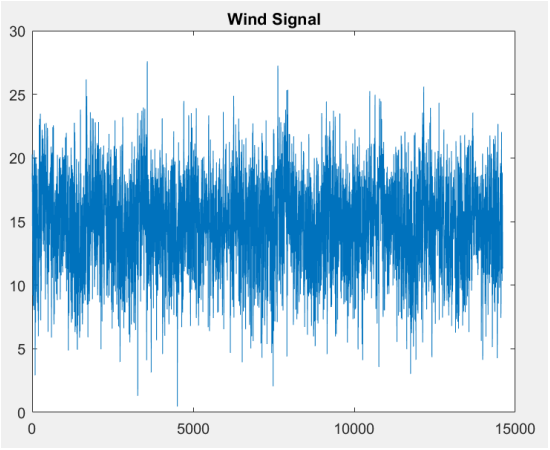

Figure 2.4. Wind data

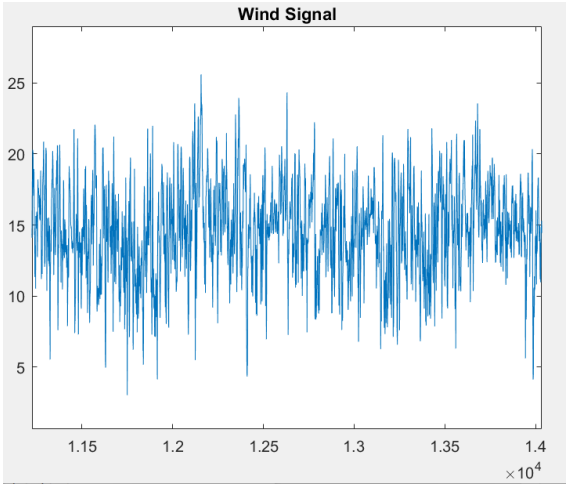

Figure 2.5. Zoom in of the wind data

This is the plot of wind data collected from internet. As shown in the graph, it is a quite random and non-stationary process. Applying EMD to such data, the result is shown below.

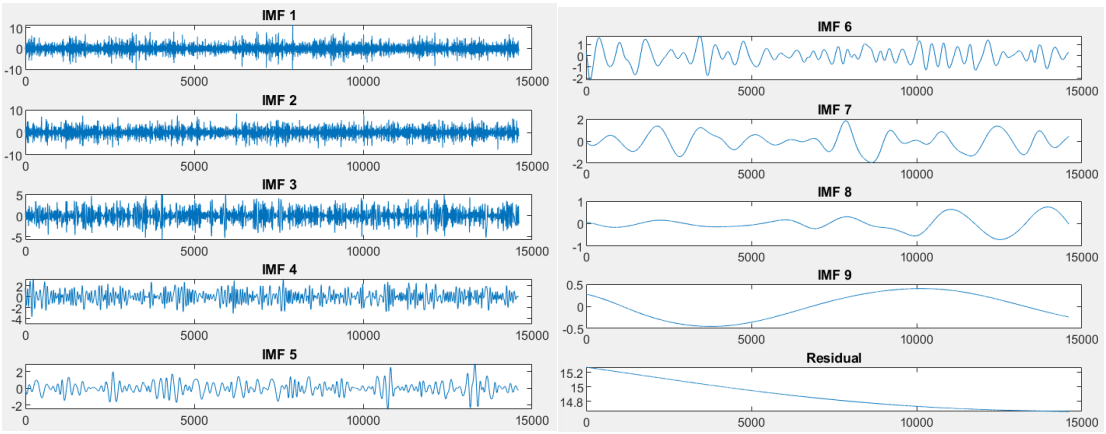

Figure 2.6. EMD results of wind data

The IMFs are obtained from the repeated sifting process as explained in previous paragraph. As the wind data is very complicated with many local extrema, it is a good example to show the efficiency of EMD because the expansion of such turbulent data can be done with only nine components. The results are already very clear as the smaller numbered IMF contains the larger frequency component from the input signal.

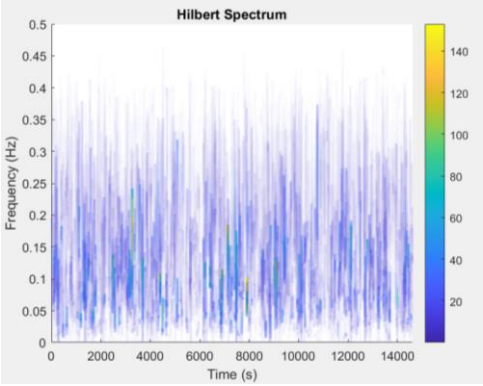

Figure 2.7. Hilbert spectrum of wind data

Another replication experiment that is pretty representative is the case of linear sum of two cosine waves as written by this expression as discussed in Huang's paper [10].

$$x(t) = 5\,cos\left(\frac{2\pi}{30}t\right) + 10\,cos\left(\frac{2\pi}{34}t\right) \tag{5}$$

The overall view of this signal is shown in this graph which is matched with the graph from the paper [10].

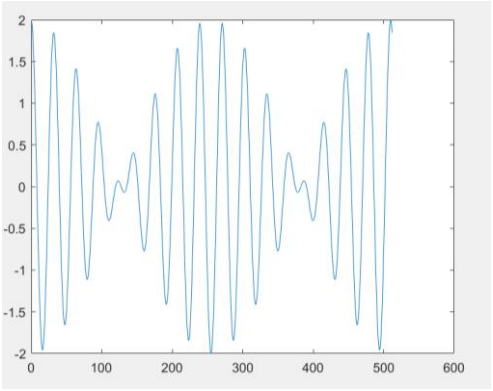

Figure 2.8. Linear sum of two sinusoidal

The property of this input signal is that the two cosine waves have very close frequencies. Therefore, in order to explicitly extract two frequency components out from the mixed signal, the tolerance of EMD decreases. With smaller threshold value or tighter stopping criterion, the algorithm would increase iterations in order to find the more precise modes.
The obtained result is shown below.

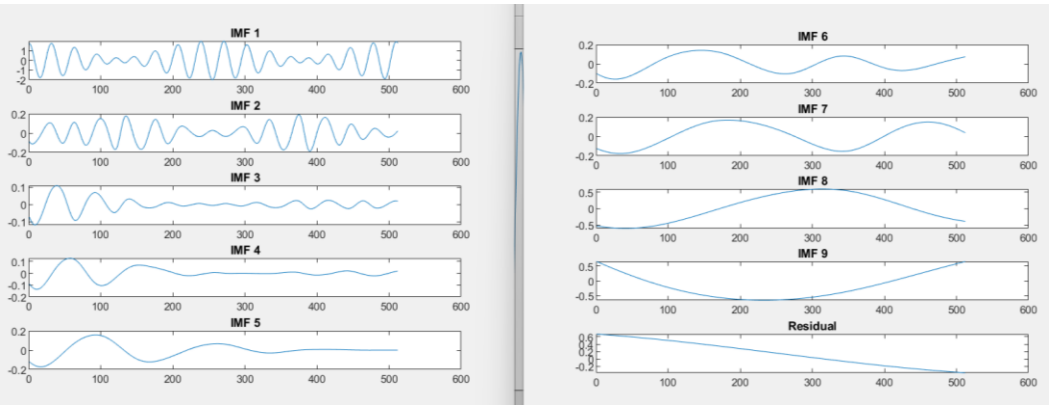

Figure 2.9. EMD results of linear sum

The first component IMF1 has 17 waves which is the result of 512/30. 512 is the total sample number and the sampling frequency is assumed to be one for simplicity. 1/30 is the frequency of the first term. Because it is a little bit larger than the frequency of the second term, it is being extracted out first. The second component IMF2 has 15 waves which is the result of 512/34 in which 1/34 is the frequency of the second cosine term. Starting from IMF3, the rest of components have much smaller energy which can be visualized by the amplitude of signals in the graph.

Next, the reconstructions of signal from IMFs are presented in the figure. The reconstructed signal is plotted in solid line while the original data is shown in dotted line.

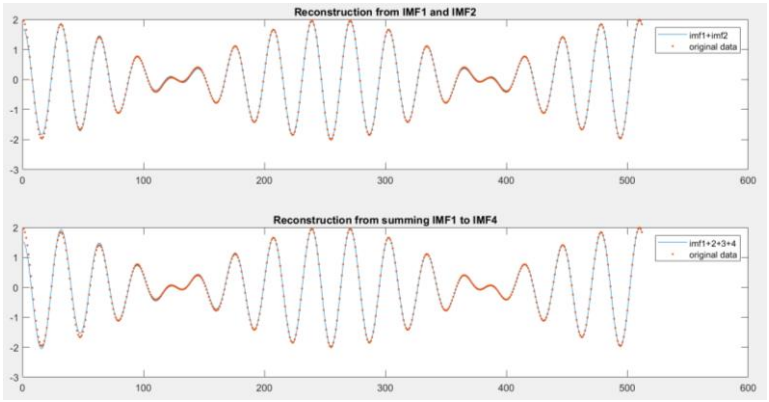

Figure 2.10. Comparison of reconstructions with original input data

The upper graph shows the comparison between original input signal x(t) and the reconstruction using IMF1+IMF2. Since in this scenario, the most of energy is contained in the first two components as illustrated in the graph for EMD result, the difference between original signal and summation of IMF1 and IMF2 is already very small. The lower graph shows the comparison between original signal and reconstruction through adding first four components IMF1 to IMF4. It has negligible difference except at the beginning which is due to the end effects.

The end effect of EMD is a remarkable swing which happens at the endpoints of the signal. Since the endpoints of the signal might not be local extrema in the decomposition of signals

that are non-stationary and non-linear, they are not captured by the envelopes. The upper envelop captures local maxima while the lower envelop captures local minima. Besides, the cubic spline interpolation method which is used to compute the envelop curve may cause the appearance of significant variation at the two ends of the interpolation signal, which would gradually spread to the middle part of the signal and in turn distort the original features of the signal along with EMD decomposition [11, 12]. Therefore, when IMFs are used to reconstruct the input data, there would be large variation at the beginning part comparing to other parts.

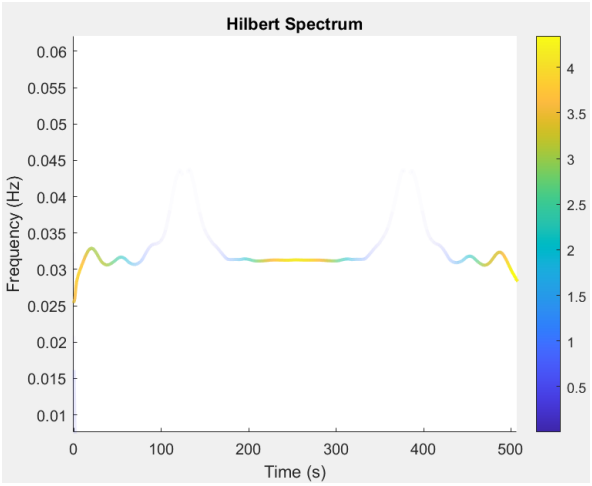

Figure 2.11. Hilbert spectrum

Putting the obtained IMFs to Hilbert spectrum, the frequency is centered at around 0.03 with certain variation according to time. This is the result of 1/30 = 0.03. The variation is caused by 1/34 = 0.029. The computed IMFs have large energy concentrated at the beginning, the middle, and the end of the graph according to the color code. This result matches with expectation since as shown in the plot of x(t), the input signal has the largest amplitude at these locations.
Sound wave is also a classical situation to apply EMD algorithm.

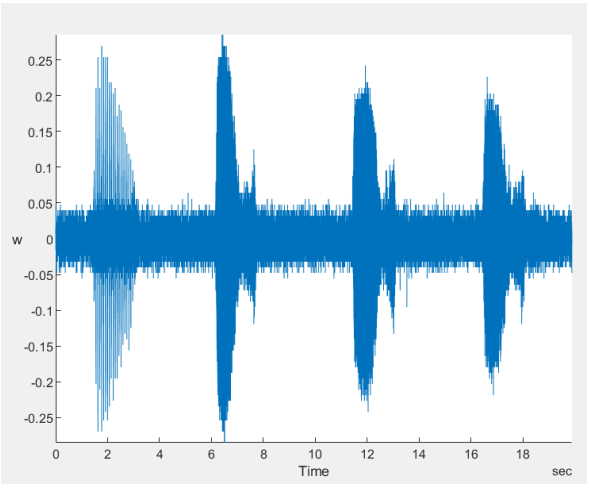

Figure 2.12. Voice sound of whale blue

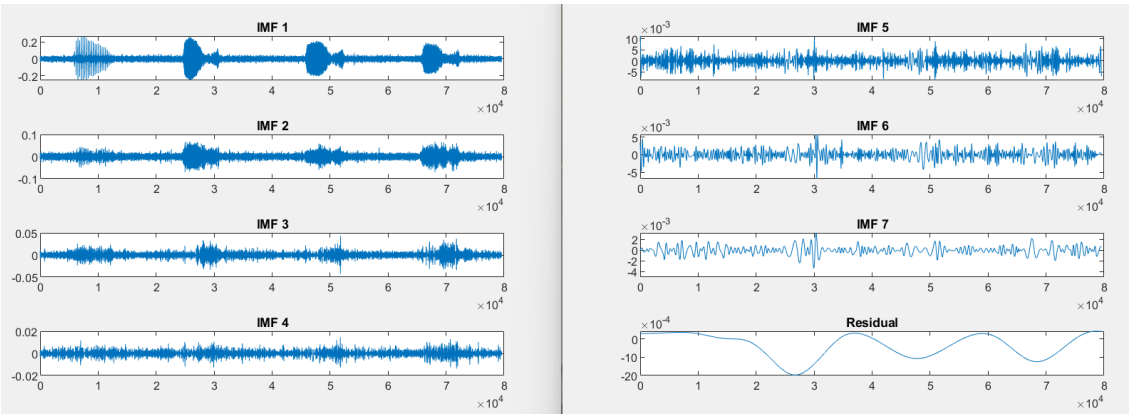

Figure 2.13. EMD results of sound wave

There are four periods of sound with high amplitude and this is the result as there are four roars of blue whale captured in the sound data. With EMD, the first period of sound is being extracted out faster than the other three periods. In IMF2, the last three periods still have quite high amplitude while the first period is much flatter. This observation can be facilitated by the Hilbert spectrum.

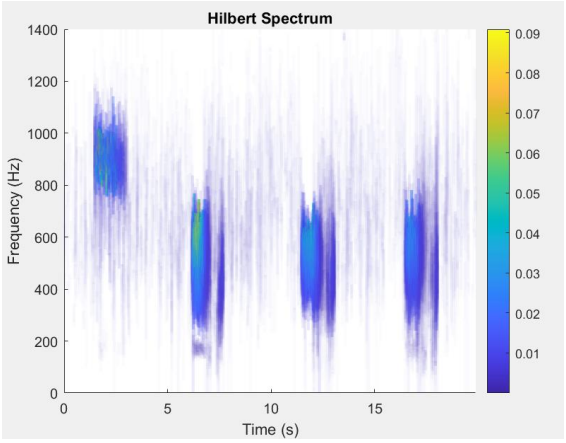

Figure 2.14. Hilbert spectrum of blue whale sound wave

With Hilbert Huang Transform, it clearly indicates that the first period or the first roar of whale has higher frequency comparing to other three periods. Hence, it is being extracted out firstly.

Until now, the functionality and the capacity of EMD algorithm to handle non-linear and non-stationary data have been well revealed.

Separating Respiration from heartbeat:

This section will give a close look at the method our team used to extract breath from the original heartbeat signal. Several assumptions are made to generate the initial parameters according to the paper we previously studied: Firstly, Breath is a signal serving as offset with a major power in frequency between 0.1 and 0.5Hz. Secondly, heartbeat is the major signal

with a frequency of 1-2Hz. Thirdly, the heartbeat does not have much vertical shifting across the periods. The breath noise will serve as the major DC offset.
By selecting IMFs with average frequency in the range of breathing and applying bandpass filters to IMFs with average frequencies slightly different from the targeted range, we have developed a system that successfully extracts out breath signals with low MSE and error rates. Based on the work we have done, we further explored the influence of each variable including the filtering range where we extract the entire or partial signal, the stopping criteria we use to control the total number of IMFs, and compared the overall performance of the selective filtering method that directly adds a bandpass filter at the system output. We used two datasets for verification: the R dataset [14] contains 5-second signals sampled at 1000 Hz frequency with a large DC offset caused by breathing for visual displaying and the B dataset [15] with 17 data at 3700Hz sampling frequency and samples for 4 minutes for the numerical computation.

In actual practice, we want to extract the signal with higher quality from the data. Due to the existence of high-frequency noise in the heartbeat signal we collected, extracting breath is a better method. Because we use dataset R for error calculation, the error between extracted and actual breath also represents the error in the extracted heartbeat signal.

The entire process of extracting breath contains five steps:
1. Using EMD to separate the original signal
2. Measure the average frequency of IMFs
3. Extract IMFs within the frequency range of respiration
4. Remove extracted IMFs from the heartbeat
5. Do bandpass filtering to the summed IMF to get the desired result
We will discuss the details of these steps in the following sections.

Mean frequency [13]:
The calculation of the average frequency for one IMF is based on the power spectral density. The algorithm firstly calculates the PSD over frequency and then it calculates the average frequency as:

The algorithm may be substituted by other methods including calculating the average distance between local minima and maxima. The detailed comparison will be shown later.

IMF extraction:
IMF extraction is the process by which we extract respiration signals from each IMF and add the extracted signals together to regenerate the original breath signal. There are two ways for IMF extraction: complete extraction and partial extraction.

Complete extraction refers to the process by which the algorithm extracts the entire IMF if the IMF average frequency lies inside the frequency range of the breath signal.

Partial extraction refers to the process in which the algorithm puts the IMF into a bandpass filter and adds the filter output to the accumulative extraction result. We will apply partial

extraction to the IMFs with an average frequency close to the extraction range for full extraction.

Further modification:

After the total extraction is obtained, it is possible to apply an extra bandpass filter at the final output to achieve less total distortion. However, this is equivalent to adding a bandpass filter to the complete extraction process. Theoretically, the extra filter should have a wider frequency range than the respiration range to maintain the high-frequency features.

Measurement of good:

Two major methods are applied to measure the effectiveness of the algorithm, MSE and average error. We use the average error calculated by the means of absolute difference over absolute value. A smaller average error represents a smaller distinction between the original and extracted results. The error is calculated between the breath signal before mixing and the extracted breath signal.

Simulation results:

The simulation result is based on the average Error collected from 20 datasets, including the results with different numbers of IMFs controlled by the stopping criteria, the results based on different bandwidths for complete extraction, and the bandpass filter range we use at the final output.

First, we compare the results from different partial extraction ranges, that is the range of IMF average frequency where we apply a bandpass with bandpass frequency [0.1,0.5] Hz. In the original result, there are outliers with error >0.4. We re-examined the data and decided to remove them due to their low data quality. The results below are generated after removing outliers where error >0.4.

Without partial extraction:

Table 1. Average error when no partial extraction is applied

Stop criteria	5e-1	2e-1	1e-2	1e-3	1e-4	1e-7
Average error	0.1769	0.1070	0.1377	0.1865	0.1384	0.1518

With partial extraction, full extraction range [0.1 0.5], partial extraction range [0.05,0.1], [0.5,1]:

Table 2. Average error when applying small range partial extraction

Stop criteria	5e-1	2e-1	1e-2	1e-3	1e-4	1e-7
Average error	0.1446	0.0919	0.1060	0.1220	0.1142	0.1425

With partial extraction, full extraction range [0.1 0.5], partial extraction range [0.025,0.1], [0.5, ∞]:

Table 3. Average error when apply broad range partial extraction

Stop criteria	5e-1	2e-1	1e-2	1e-3	1e-4	1e-7
Average error	0.1431	0.0935	0.1049	0.1212	0.1165	0.1391

We can observe that applying the bandpass for IMFs reduces the total distortion. When the stopping criteria are too large, the error increases due to not enough IMFs within the range, and when it is too small, the error also becomes larger since merging too many IMFs might cause the addition of unwanted noises. According to simulation results, the best results are obtained when doing partial extraction for IMFs in the range [0.05,0.1], [0.5,1] and stopping criteria at 2e-1. Based on these results, we further investigate the influence of the frequency range for partial and full IMF extractions (we must change these two bandpass frequencies together otherwise it will be meaningless):

Table 4. Average error with different extraction frequencies when apply small range partial extraction

Full extraction frequency	[0.1,0.6]	[0.1,0.5]	[0.05,1]	[0,1]
Average error	0.0896	0.0919	0.0964	0.1017

Different from our initial assumption, the signal power is concentrated in a slightly wider range. However, it did not differ from our initial assumptions. Therefore, we adjusted the extraction range to be larger (0.1,0.6).

Simulation plots:

Beyond the numerical error we compute, the actual shape we obtain is also important. With these new modifications, we plot the breath extraction results for data in each dataset, and the resulting plots are shown below:

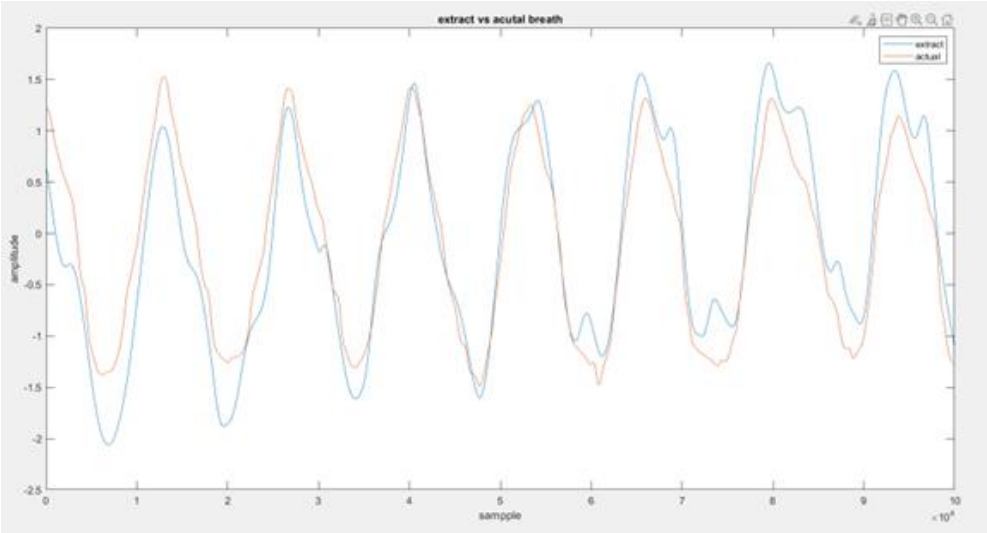

Fig. 3.1.1 (a) Dataset B extraction result

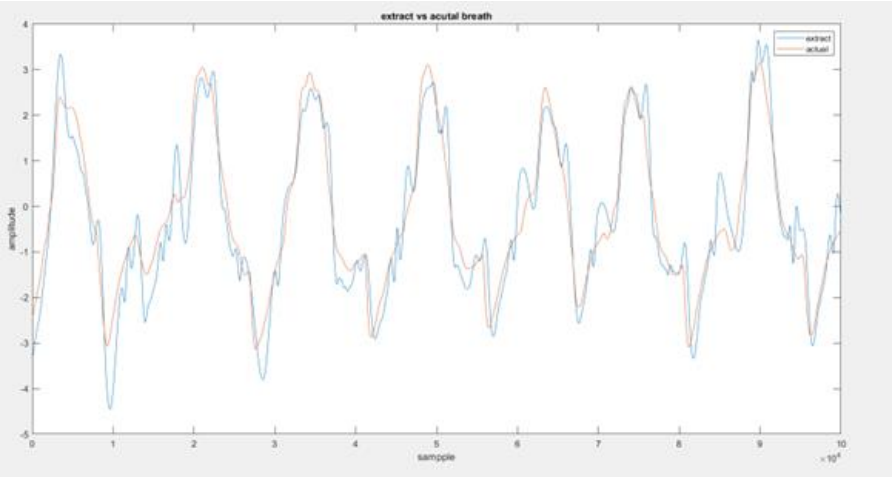

Fig. 3.1.1 (b) Breath input from two different data

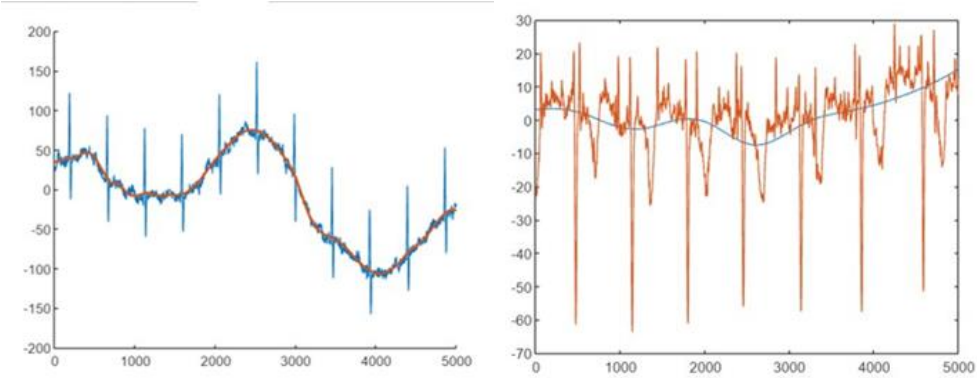

Fig. 3.1.2 Dataset R extraction result vs mixed input from two different data

From data set B's extraction result, we can observe that the major features of the frequency are retained with a slight amount of high-frequency noise. And from dataset R's result, we can observe the low-frequency R is nicely extracted from one breath.

Compared to adding the bandpass filter directly to the output:

As we introduced in the final presentation, directly adding a bandpass filter to the IMFs is equivalent to using a bandpass filter to realize the extraction. This results in more noise and loss in terms of high-frequency features. The following three plots show that our method is superior when comparing extracted results to actual input:

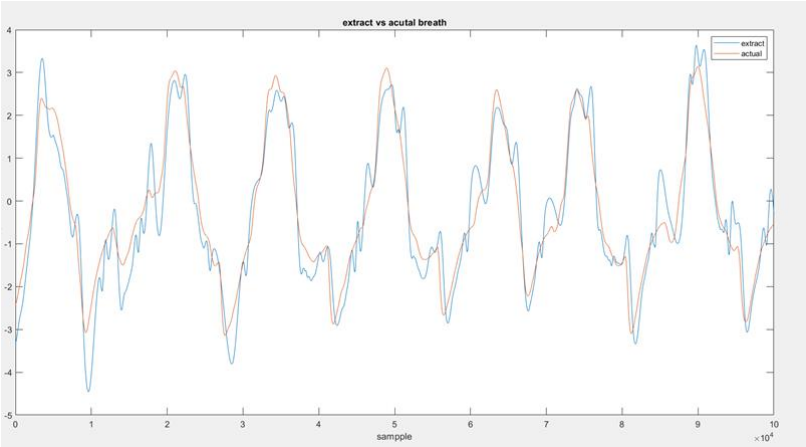

Fig 3.2.1 Extracted results using partial filtering (error = 0.03)

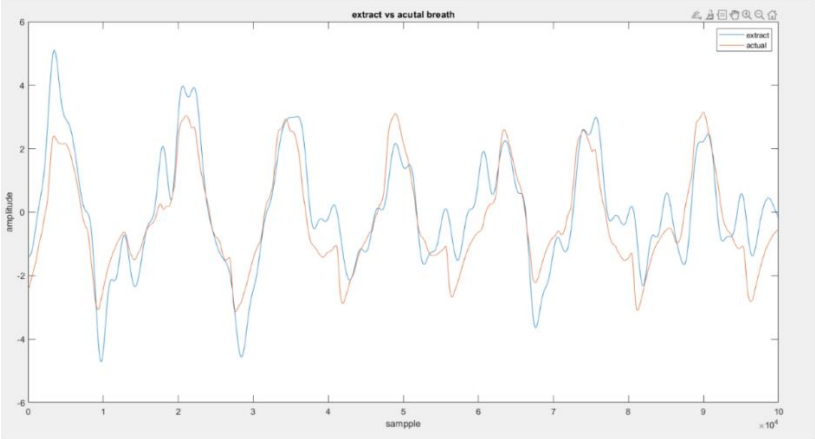

Fig 3.2.2 Extracted results using bandpass filtering for the range [0.2,1.5] (error=0.07)

We tried multiple bandpass frequencies and selected the best one for presentation. The bandpass filter causes distortion and loss in high-frequency features of the original signal. It also causes more errors numerically. Although it partially purifies the high-frequency noises, it causes significantly more distortions to the system.

Conclusion:

In conclusion, EMD is a useful method that can extract a signal with most of its power at low frequency but with large bandwidth from a wideband higher–frequency signal. Using our method, we found a good method that can maintain the shape of high-frequency parts while extracting out the breath signal with low error.

To further improve the algorithm, one might conduct IRR filtering or other methods to remove the high frequency noise from the original signals and improve the overall signal quality. It is also possible to utilize machine learning and other algorithms to find best parameters for partial and complete extraction basing on the HHT diagrams generated by the IMFs. From the work we have completed, we see great potential in using EMD to extract breath signals from heartbeats.

References

[1] Barold SS. Willem Einthoven and the birth of clinical electrocardiography a hundred years ago. Card Electrophysiol Rev. 2003 Jan;7(1):99-104. doi: 10.1023/a:1023667812925. PMID: 12766530.

[2] Ashley EA, Niebauer J. Cardiology Explained. London: Remedica; 2004. Chapter 3, Conquering the ECG. Available from: https://www.ncbi.nlm.nih.gov/books/NBK2214/

[3] Sattar Y, Chhabra L. Electrocardiogram. [Updated 2023 Jun 5]. In: StatPearls [Internet]. Treasure Island (FL): StatPearls Publishing; 2023 Jan-. Available from: https://www.ncbi.nlm.nih.gov/books/NBK549803/

[4] Wei X, Yohannan S, Richards JR. Physiology, Cardiac Repolarization Dispersion and Reserve. [Updated 2022 Apr 21]. In: StatPearls [Internet]. Treasure Island (FL): StatPearls Publishing

[5] JoVE Science Education Database. Biomedical Engineering. Acquisition and Analysis of an ECG (electrocardiography) Signal. JoVE, Cambridge, MA, (2023).

[6] Balasubramanian, S. ., Naruka, M. S. ., & Tewari, G. (2023). Denoising ECG Signal Using DWT with EAVO . International Journal on Recent and Innovation Trends in Computing and Communication, 11(3s), 231–237. https://doi.org/10.17762/ijritcc.v11i3s.6184

[7] Gustavo Lenis, Nicolas Pilia, Axel Loewe, Walther H. W. Schulze, Olaf Dössel, "Comparison of Baseline Wander Removal Techniques considering the Preservation of ST Changes in the Ischemic ECG: A Simulation Study", *Computational and Mathematical Methods in Medicine*, vol. 2017, Article ID 9295029, 13 pages, 2017. https://doi.org/10.1155/2017/9295029

[8] Centeno-Bautista MA, Rangel-Rodriguez AH, Perez-Sanchez AV, Amezquita-Sanchez JP, Granados-Lieberman D, Valtierra-Rodriguez M. Electrocardiogram Analysis by Means of Empirical Mode Decomposition-Based Methods and Convolutional Neural Networks for Sudden Cardiac Death Detection. *Applied Sciences*. 2023; 13(6):3569. https://doi.org/10.3390/app13063569

[9] V. Babak, A. Zaporozhets, Y. Kuts Yurii, and L. Shcherbak, “Some features of Hilbert transform and their use in Energy Informatics,” *The Problems of General Energy*, vol. 2022, no. 1–2, pp. 90–96, 2022. doi:10.15407/pge2022.01-02.090

[10] N. E. Huang *et al.*, “The empirical mode decomposition and the Hilbert spectrum for nonlinear and non-stationary time series analysis,” *Proceedings of the Royal Society of London. Series A: Mathematical, Physical and Engineering Sciences*, vol. 454, no. 1971, p. 903?995,

Mar. 1998.

[11] T. Xiong, Y. Bao, and Z. Hu, “Does restraining end effect matter in EMD-based modeling framework for time series prediction? some experimental evidences,” *Neurocomputing*, vol. 123, pp. 174–184, 2014. doi:10.1016/j.neucom.2013.07.004

[12] D.-C. Lin, Z.-L. Guo, F.-P. An, and F.-L. Zeng, “Elimination of end effects in empirical mode decomposition by mirror image coupled with support vector regression,” *Mechanical Systems and Signal Processing*, vol. 31, pp. 13–28, 2012. doi:10.1016/j.ymssp.2012.02.012

[13] “Luscinia.” *Mean Frequency*, luscinia.sourceforge.net/page26/page35/page35.html. Accessed 8 Dec. 2023.

[14]Jezewski J, Matonia A, Kupka T, Roj D, Czabanski R. >Determination of the fetal heart rate from abdominal signals: evaluation of beat-to-beat accuracy in relation to the direct fetal electrocardiogram. Biomedical Engineering/Biomedizinische Technik 2012 Jul;57(5):383-394. doi:10.1515/bmt-2011-0130.

[15] García-González, M.A.; Argelagós-Palau, A.; Fernández-Chimeno, M.; Ramos-Castro, J., “A comparison of heartbeat detectors for the seismocardiogram,” Computing in Cardiology Conference (CinC), 2013